Improving resist resolution and sensitivity via electric-field enhanced postexposure baking

Mosong Cheng,[a] Lei Yuan, Ebo Croffie, and Andrew Neureuther
Electronics Research Laboratory, University of California, Berkeley, California 94720-1772

(Received 11 June 2001; accepted 4 February 2002)

This article explores a methodology for enhancing the resist resolution and improving resist profile based on confining the photoacid drift/diffusion by an external electric field. A properly offset alternating electric field applied to the resist film during postexposure bake (PEB) can enhance the photoacid drift in the vertical direction, drive acid to the desired direction, and thereby confine the lateral acid diffusion. The experiments were conducted on UVIIHS resist with JEOL electron-beam exposure tool and UVII-10 resist on ASML KrF stepper, respectively. The scanning electron microscopy pictures show that electric-field enhanced PEB can control the resist profiles and increase the verticality of resist sidewalls. Electric-field-enhanced PEB also significantly improves the tolerance of over and underexposure and provides better critical dimension control. It is estimated that it reduces the lateral acid diffusion length by about 70–90 nm in KrF lithography.
 [DOI: 10.1116/1.1464835]

I. INTRODUCTION

Chemically amplified resists are based on the acid catalyzed deprotection of functioning groups in a polymer matrix. During the postexposure bake (PEB) step, several chemical and physical processes take place. Photoacid catalyzes the de-blocking process,[1] in which the blocked insoluble polymer is converted to a soluble polymer with hydroxyl group and a volatile component. The volatile group then generates free volume that enhances the photoacid diffusivity. Meanwhile, the photoacid can be deactivated by neutralization and evaporation, or be trapped due to lack of free volume. Some resist systems also suffer from substrate or air contamination.[1]

The photoacid is composed of a negatively charged anion and a positively charged proton. Based on the fact that it is the proton that catalyzes the de-protection reaction,[2] a methodology termed ''electric-field-enhanced postexposure baking'' (EFE-PEB) was proposed in Ref. 3 to improve resist resolution and sensitivity by applying an alternating electric field across the resist film during PEB to enhance the proton drift at vertical direction. The anion is separated from H+ ion during PEB and its mobility is negligible compared with H+, therefore the impact of electric field on anion can be ignored in the EFE-PEB process. Prior art on the application of electric fields during PEB to control and improve resist profiles in a pair of patents by Tokui and Yoneda[4] was brought to our attention during the review process for this article. Tokui and Yoneda, who used a dc field of 10–100 kV/mm on SAL-601-ER-7, described the preferred movement of the H^+ downward from an attenuated KrF exposure, and gave a schematic diagram of the resulting resist profile improvement rather than SEMs of resist profiles. Direct SEM evidence of improved resist profiles and improved critical dimension (CD) tolerance was given by the current authors for the EFE-PEB treatment of electron-beam exposures in Ref. 3. It is believed that the alternating direction of the field leads to an order of magnitude greater arc length of the H^+ in the material and hence a resist profile improvement effect that is easier to observe. In this article, the EFE-PEB method as developed by the current authors is further explored to control resist profiles by manipulating the field polarity and magnitude. Experiments on both electron-beam and KrF lithography are described and discussed.

II. POSTEXPOSURE BAKE MODEL

The postexposure bake processes under the influence of electric field can be described by the following partial differential equations:[5]

$$\frac{\partial C_{\mathrm{as}}}{\partial t} = K_1(1 - C_{\mathrm{as}})C_a, \tag{1}$$

$$\frac{\partial C_a}{\partial t} = \nabla.(D\nabla C_a) - \nabla.(\mu \mathbf{E} C_a) - K_2 C_a. \tag{2}$$

C_{as} is the activated site concentration, defined as the percent of blocking groups that have been deblocked. C_a is the acid concentration. Equation (1) demonstrates the acid-catalyzed de-protection reaction and Eq. (2) describes the acid diffusion, loss, and drift in the presence of an electric field.

The acid mobility μ is related to acid diffusivity D by the Einstein equation

$$\mu = \frac{qD}{kT}, \tag{3}$$

where q is the charge of the proton.

To improve the resist profile, it is desired to enhance the acid drift in the vertical direction and reduce the acid diffusion in the horizontal direction. Hence the electric field is applied along the vertical direction, as is illustrated in Fig. 1.

The photoacid distribution profiles after EFE-PEB are plotted in Fig. 2, assuming $D = 50\ \mathrm{nm}^2/\mathrm{s}$, resist thickness $L = 600\ \mathrm{nm}$, PEB time 90 s, initial acid distribution is

[a]Electronic mail: mosong@eecs.berkeley.edu

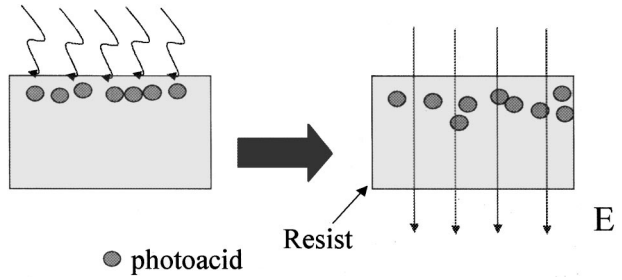

FIG. 1. Principle of electric-field-enhanced postexposure baking. The acid is generated in exposure, and its drift in the vertical direction is enhanced by electric field.

$C_a(x,y,z,0)=C\delta(x)\delta(y)z$. Here we assume z is the vertical direction, $z=0$ corresponds to the bottom of resist while $z=L$ corresponds to the top of resist. In Fig. 2(a), from left to right are the acid distribution profiles corresponding to $V=0$, 0.2, and 0.3 V, respectively, where V is the voltage drop from the top to the bottom of the resist film. It can be seen that the standard PEB can hardly improve the acid distribution uniformity while the 0.2 V EFE-PEB can significantly smooth the acid distribution. If the voltage is as high as 0.3 V, however, the majority of acid will be shifted to the bottom of resist by the electric field. Figure 2(b) compares the acid distribution after PEB along the **x** axis, which is a lateral direction. For the standard PEB ($E=0$ V/m), the acid distribution is taken at $z=L$, where the acid spreads farthest laterally. For the EFE-PEB ($E=3.3\times10^5$ V/m, or $V=0.2$ V), the acid distribution is taken at $z=L/2$, where the lateral diffusion of acid is largest. It can be seen that the EFE-PEB has a smaller amount of acid diffusing laterally than standard PEB does, due to the fact that EFE-PEB can average the vertical acid distribution.

The dissolution rate of resist is determined by C_{as}, activated site concentration. Solving Eq. (1), C_{as} is given by

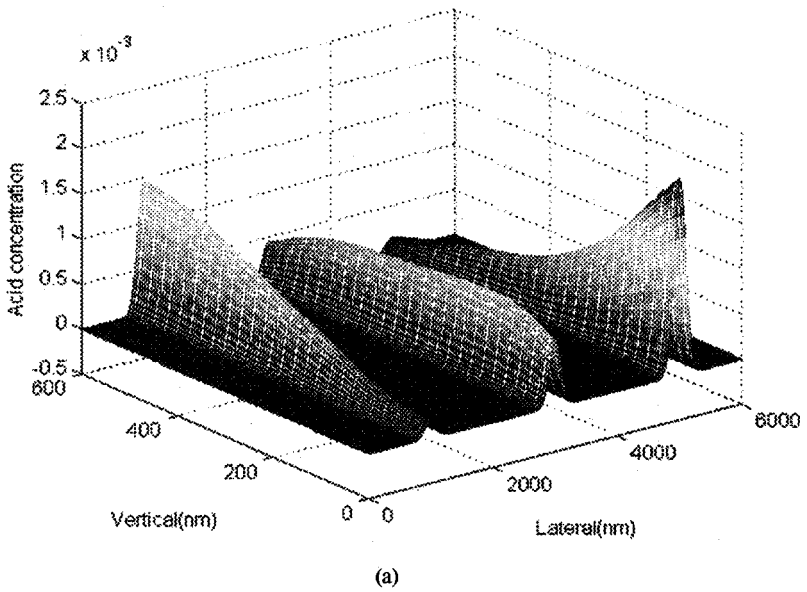

(a)

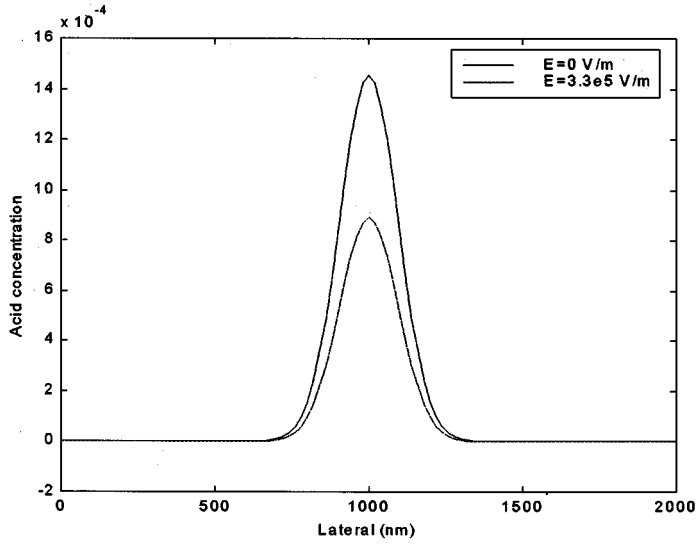

(b)

FIG. 2. Photoacid distribution after PEB. In (a), from left to right are the acid distribution corresponding to standard PEB, 0.2 and 0.3 V EFE-PEB. (b) Acid lateral diffusion after standard PEB and 0.2 V EFE-PEB.

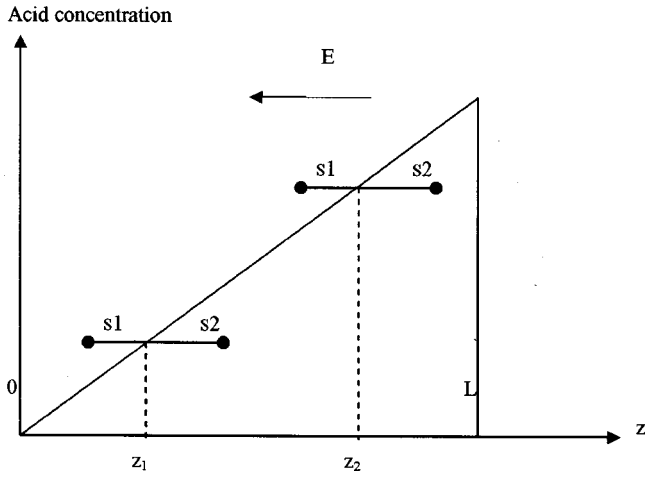

FIG. 3. One-dimensional EFE-PEB model. Initial acid concentration linearly decreases from $z=L$ to $z=0$. The direction of constant electric field **E** is negative. Any point z can be visited by acid from $[z-s_1, z+s_2]$. Note that $s_1<s_2$.

$$C_{\text{as}}(x,y,z,t)=1-\exp\left(-K_1\int_0^t C_a^m(x,y,z,\tau)d\tau\right). \tag{4}$$

To improve the resist profile, we want to obtain a vertically uniform activated site concentration. From Eq. (4), C_{as} at a certain point is determined by the amount of acid passing through this point during PEB. Optical radiation of resist yields more photoacid at the top and less at the bottom due to resist absorption. A downward electric field can help migrate photoacid towards the bottom, thus results in a better resist profile. A direct field, however, is not sufficient to obtain a uniform activated site concentration, and is not efficient in driving acid-catalyzed de-protection. To illustrate this, consider a one-dimensional model depicted in Fig. 3. The acid concentration linearly decreases from $z=L$ to $z=0$, and the electric field **E** also points from $z=L$ to $z=0$. Assume **E** and D are uniform in the resist layer. During PEB, a given point z can be visited by the drifting/diffusing acid from the interval $[z-s_1, z+s_2]$. Obviously $s_1<s_2$, and s_1, s_2 do not depend on z. Thus if $z_1<z_2$, the amount of acid in interval $[z_1-s_1, z_1+s_2]$ is smaller than in interval $[z_2-s_1, z_2+s_2]$. As a result, $C_{\text{as}}(z_1)$ will be smaller than $C_{\text{as}}(z_2)$ after PEB. On the other hand, if $z_1+s_2>L$ and $z_2+s_2>L$, in the case of large **E**, then z_1 and z_2 are visited by acid from $[z_1-s_1, L]$ and $[z_2-s_1, L]$, respectively. Thus $C_{\text{as}}(z_1)$ will be greater than $C_{\text{as}}(z_2)$. To make C_{as} identical everywhere, a simple solution is to make s_1 and s_2 so large that any point can be visited by acid from interval $[0, L]$. Note that s_1 can only be increased by an upward electric field. Thus an alternating field, rather than a direct field, is desired to obtain vertically uniform activated site concentration. In addition to the alternating field, a small downward direct field can also be of help by migrating the excessive acid at the top towards the bottom.

EFE-PEB with alternating field can also make the acid-catalyzed deprotection reaction more effective. In EFE-PEB, the acid ion will move much faster in the vertical direction, and it will catalyze much more de-protection reactions in the vertical direction than in the lateral direction. Compared with the standard PEB, the acid will catalyze the same number of reactions. But the increased movement of the acid in the vertical direction means that reaction events tend to occur and consume the acid along a more vertical path. This directed consumption depletes the number of catalytic events available for enabling reactions in the lateral direction and, has the effect of confining the lateral motion of the acid. It can be concluded that the lateral (unwanted) dissolution of resist will be reduced, compared with the standard PEB. Meanwhile, the vertical (desired) dissolution of resist will be enhanced due to more vertical acid motion. Thus the EFE-PEB can aggressively modify the resist profile.

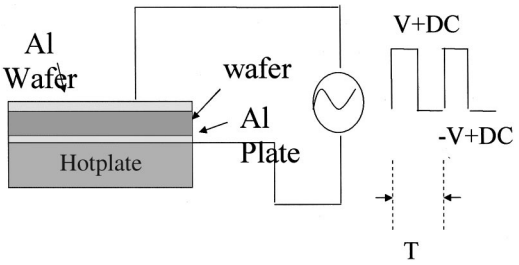

FIG. 4. Setup of electric-field-enhanced PEB. The wafer is in between two Al sheets, to which the cathodes are connected. The wave form of the output voltage is shown on the right side. It is a bipolar rectangle wave with peak voltage $V+\text{dc}$ and $-V+\text{dc}$, and period T, where dc is the dc offset.

From Eqs. (2) and (3), a large **E** and a short PEB time are desired. To enhance the vertical de-protection and reduce the lateral de-protection by transporting acid, an alternating electric field with an offset bias is needed. The frequency and offset bias should be adjusted based on the acid diffusivity and different amount in the exposed/unexposed area.

The electric-field-enhanced PEB setup and the voltage wave form are shown in Fig. 4. Note that the voltage in the first half period is $V+\text{dc}$ and in the second half period, it is $-V+\text{dc}$. The dc offset bias is dc while the ac component is V.

III. EXPERIMENT SETUP

The first set of experiments was conducted on a JEOL electron-beam exposure tool. The resist UVIIHS was coated on highly doped wafers (the resistance is $<10\ \Omega$, hence the voltage drop across the substrate can be ignored) at 3000 rpm for 30 s and soft baked at 140 °C for 60 s. The exposure doses were 7, 9, 12, 16 μC/cm^2 with beam currents 5 and 10 pA. The patterns of equal line/space (L/S) were exposed, and the line/space widths were 100, 200, and 300 nm, i.e., $L/S=100/100$, 200/200, 300/300 nm. To exclude the environmental variations, we always loaded two chips into the exposure tool at the same time. Even though e-beam exposure has to be conducted in a sequential manner, the second chip was always exposed within 20 min after the first chip was exposed. Since the exposures were conducted more than 2 h after tuning the exposure tool, it is believed that the beam current drift was ignorable. Both chips were exposed with

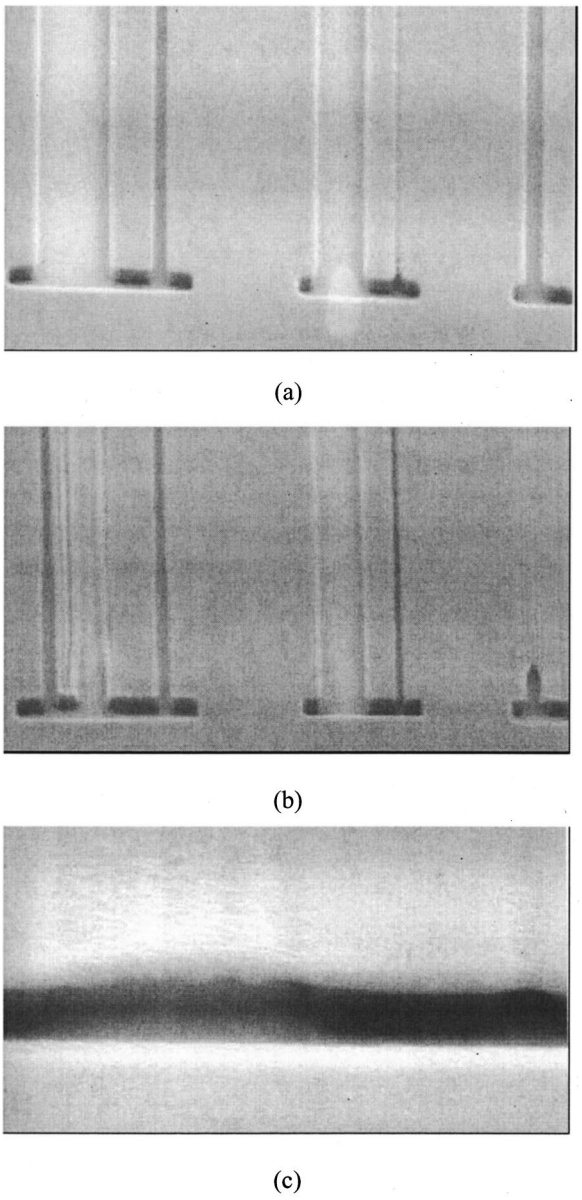

FIG. 5. Comparison of upward/downward EFE-PEB and standard PEB for 0.3, 0.2, and 0.1 μm L/S, dose 12 μC/cm^2. (a) Standard PEB. (b) EFE-PEB, dc upward. (c) EFE-PEB, dc downward, only 0.3 μm L/S is shown in (c).

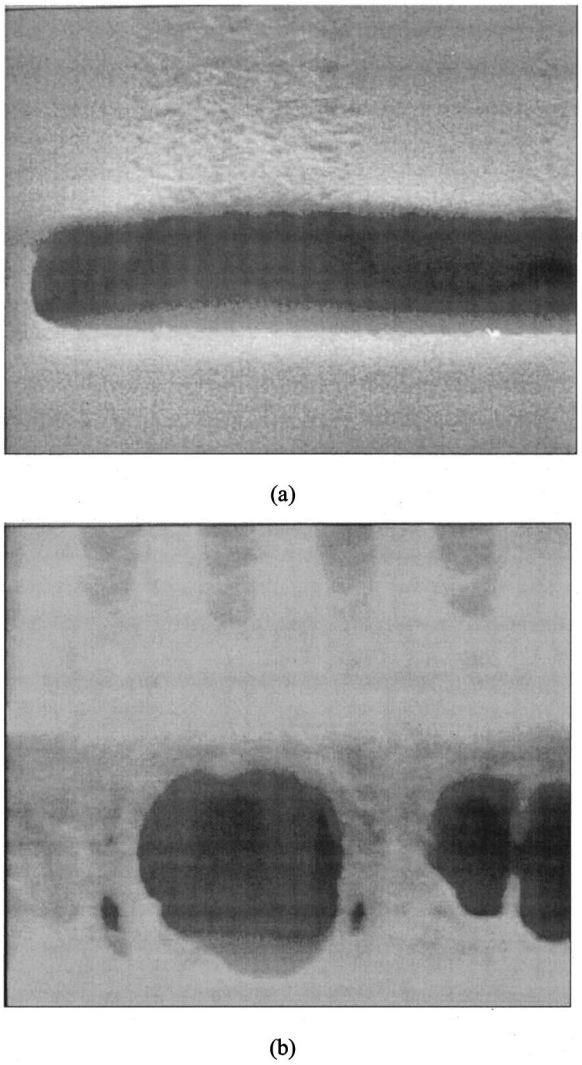

FIG. 6. Comparison of EFE-PEB and standard PEB for 0.2 μm L/S, dose 9 μC/cm^2. (a) Standard PEB, 140 °C, 90 s. (b) EFE-PEB dc upward.

the same dose/beam current matrix. Then one chip was randomly chosen for EFE-PEB and the other for standard PEB. The standard PEB conditions are: 140 °C, 90 s. Two sets of EFE-PEB conditions were: 140 °C, frequency 3 Hz, dc 0.65 V, ac 6.5 V, 90 s, with the dc direction from the bottom to the top of the resist layer (upward) and from the top to the bottom of the resist layer (downward). Note that in standard PEB, the Al wafer was also placed on the resist top to eliminate the thermal difference between standard PEB and EFE-PEB. Finally, the chips were developed in 0.263N tetramethylam moniumhydroxide (TMAH) for 60 s at room temperature.

The second set of experiments was done on an ASML KrF stepper. The resist UVII-10 was coated on 6 in. wafers. Though the wafers were not highly doped, their conductivity was much higher than that of the resist so that the voltage drop across the wafers could be neglected. The resist processing parameters are: spin 6000 rpm for 30 s, soft bake 130 °C for 90 s, exposure dose 27 mJ/cm^2, NA 0.5, σ 0.2. Dense line/space with different pitches were exposed. Since the resist profiles at different pitches were consistent, only the data of $L/S=400/400$ nm are presented in this article. On a 6 in. wafer, 26 dies of 2.1 cm$\times$2.1 cm were exposed with the identical dose of 27 mJ/cm^2. During PEB, a 4 in. Al wafer was placed on the 6 in. wafer, covering half the dies. Thus half the dies were applied electrical field while the other half were on standard PEB. In EFE-PEB, the Al wafer was preheated to 130 °C so that the thermal perturbation induced by Al wafer was diminished. By use of this approach, the EFE-PEB and standard PEB can be considered to have identical thermal histories. The standard PEB is 130 °C, 90 s. Again, two sets of EFE-PEB were tested with frequency 2.5 Hz, ac 6.5 V, dc 6.5 V, dc upward and dc downward. Finally the wafers were developed in 0.263N TMAH for 60 s at room temperature. In both e-beam and deep ultraviolet

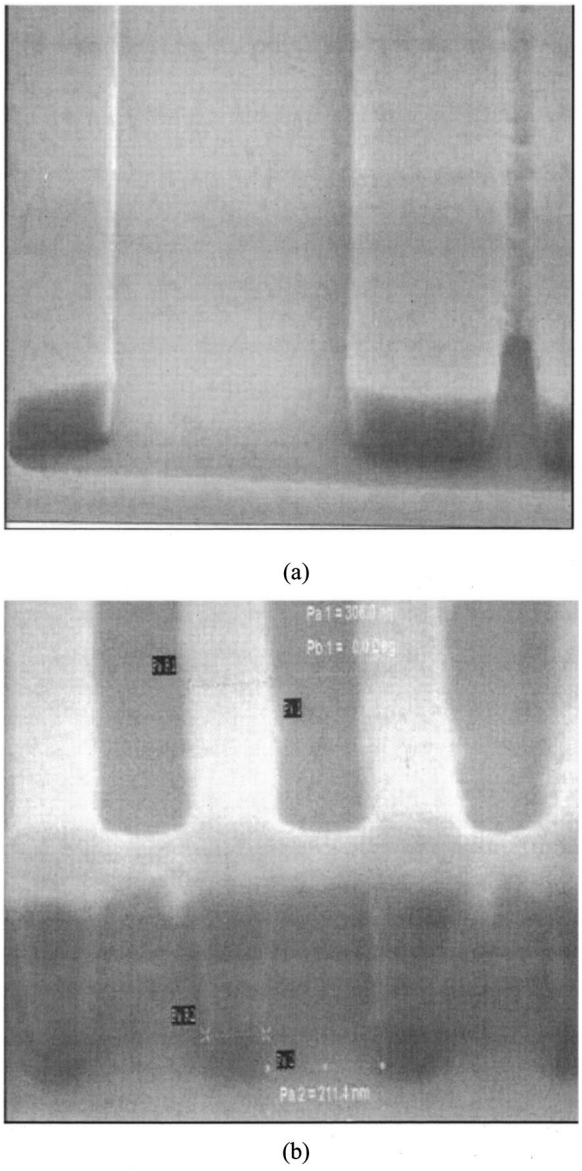

FIG. 7. Comparison of EFE-PEB and standard PEB for 0.3 μm L/S, dose 9 μC/cm^2. (a) Standard PEB. (b) EFE-PEB, dc upward.

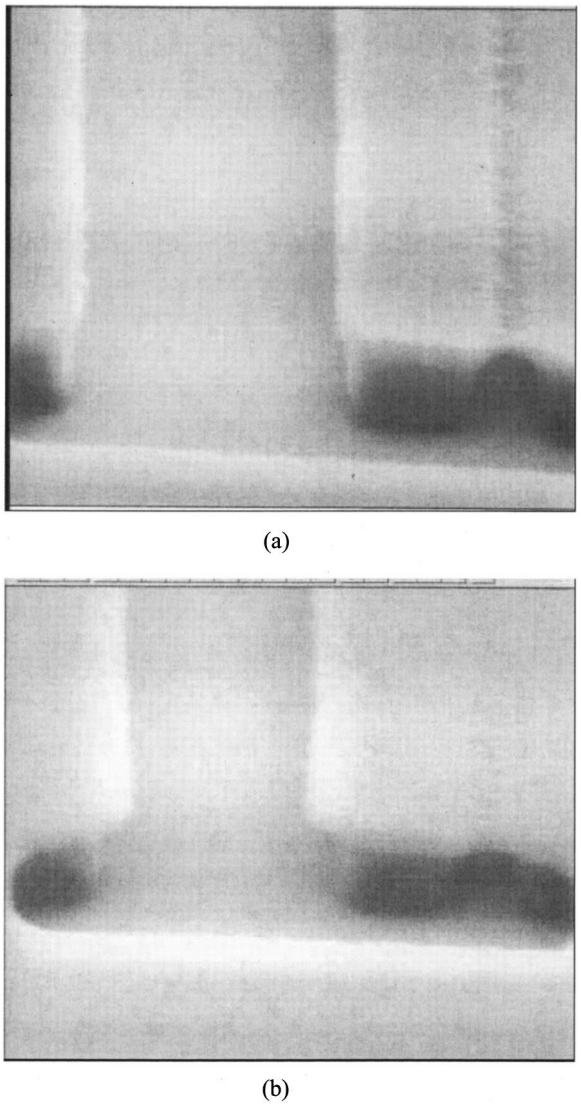

FIG. 8. Comparison of EFE-PEB for 0.2 μm L/S, dose 16 μC/cm^2. (a) EFE-PEB with 3 Hz, 9.8 V ac, 0.65 V dc, upward. (b) EFE-PEB with identical frequency and voltage, but dc downward.

(DUV) experiments, a very important treatment of the Al wafer, which is the cathode, was to coat it with an insulating thin film. The film is made by spinning resist on the Al wafer and baking at 300 °C for 10 min. Without this insulator, the H+ ion was found loss on the top, which is believed to be neutralized by obtaining an electron from Al in the anode. Being pressed by tweezers in PEB, the Al cathode has good contact with the resist film.

IV. EXPERIMENTAL RESULTS AND ANALYSIS

The process of UVIIHS resist is not optimized for e-beam lithography, and Ref. 3 indicated *T* topping taking place to some extent in e-beam experiment, which is believed due to e-beam dose distribution in resist. Thus an upward dc is expected to improve UVIIHS resist profiles. The SEM pictures show that EFE-PEB has noticeably improved the resist profile.

Figure 5 compares the tilted top view of EFE-PEB with that of standard PEB. The dose is 12 μC/cm^2. Under standard PEB, all the resist feet were undercut so severely that the lines were washed away. Under EFE-PEB with an upward dc, however, the acid was driven up without undercutting the lines so they still remained. On the other hand, the EFE-PEB with downward dc drove the acid down to the bottom of the resist, thus the *T*-top effect was made even worse so that the top of the resist still remained while the underneath part of the resist was developed and a ''comb'' was formed.

For 0.2 μm L/S shown in Fig. 6, the standard PEB resulted in a very severe *T*-top effect such that a ''comb'' was formed, as is shown in Fig. 6(a). The EFE-PEB led to the development of resist surface to some extent and all the resist

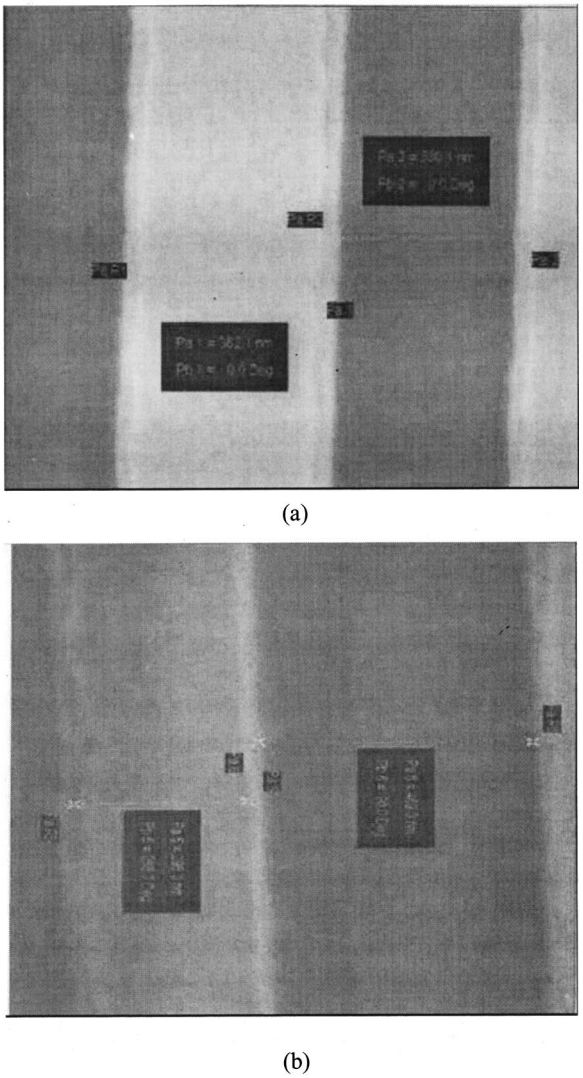

FIG. 9. Comparison of EFE-PEB and standard PEB in DUV lithography, 0.4 μm L/S, dose 27 mJ/cm^2. (a) EFE-PEB with 2.5 Hz, 6.5 ac, 6.5 V dc downward. (b) Standard PEB 130 °C, 90 s.

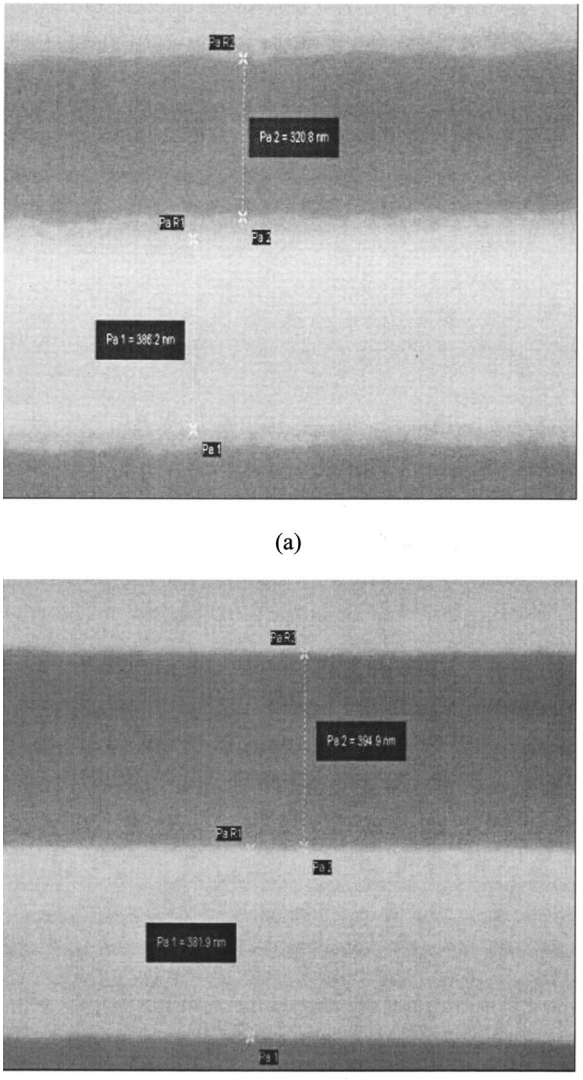

FIG. 10. Comparison of upward EFE-PEB and standard PEB in DUV lithography, 0.4 μm L/S, dose 27 mJ/cm^2. (a) EFE-PEB with 2.5 Hz, 6.5 ac, 6.5 V dc upward. (b) Standard PEB 130 °C, 90 s.

feet remained. This is a clear proof that the acid was driven to the top and implies that the EFE-PEB has better tolerance of underexposure.

Figure 7 compares the 0.3 μm L/S patterns. It can be seen that the EFE-PEB lead to a much better resist profile, even though there is some bridging effect at the resist edge. On the contrary, the standard PEB eliminated all resist lines.

Figure 8 compares the 0.2 μm L/S patterns, dose 16 μC/cm^2, which is overexposed. The upward EFE-PEB resulted in a clean sidewall. The downward EFE-PEB, however, resulted in a ''roof'' at the resist edge, which indicates a worse T-top effect due to downward acid drift. This particular set of treatment was run six times. Each time one chip was processed by standard PEB and the other by either upward or downward EFE-PEB. In all six cases, the resist profiles resulted from upward and downward EFE-PEB and showed a difference. The upward EFE-PEB always resulted in wider opening at the resist top surface than the downward EFE-PEB did.

Figure 9 compares the $L/S=400/400$ nm patterns obtained by KrF lithography. Both EFE-PEB and standard PEB lead to good resist patterns. Since no anti-reflective coating was applied and σ is small, there exists a strong standing-wave effect on the resist sidewalls, indicated by the line edges. The ac/dc of EFE-PEB was not optimized to eliminate the standing-wave effect. However, the existence of the dc field lead to a better CD. Standard PEB gave $L/S=295/469$ nm, while EFE-PEB gave $L/S=362/380$ nm, reducing the lateral deprotection length by about 90 nm.

Figure 10 compares the same patterns under standard PEB and upward EFE-PEB treatment. Since the acid at the bottom was driven away in the latter case, a narrower resist opening at the resist bottom is expected. This is confirmed by the SEM pictures, which show that the spacing at the resist bottom is 321 nm in upward EFE-PEB while it is 395 nm in standard PEB.

V. CONCLUSION AND FUTURE WORK

This article explored the methodology for enhancing the resist resolution and controlling resist profiles in electron-beam and KrF lithography based on confining the photoacid drift/diffusion by applying external electric field. Generally a high-voltage, low-frequency electric field with a properly directed dc offset is desired to optimize the resist profile. Better vertical uniformities and clean resist sidewalls were observed and, in DUV lithography, the remaining resist lines were 70–90 nm wider. The reduced lateral diffusion/deprotection significantly improve the tolerance for over- and underexposure and CD uniformity.

ACKNOWLEDGMENTS

This work is supported in part by industry and by the State of California in the SMART program SM97-01.

[1]B. Mortini *et al.*, J. Vac. Sci. Technol. B **15**, 2534 (1997).
[2]C. Mack, *Inside PROLITH: A Comprehensive Guide to Optical Lithography Simulation* (FINLE Technologies, Inc., Austin, TX, 1997).
[3]M. Cheng *et al.*, J. Vac. Sci. Technol. B **18**, 3318 (2000).
[4]Akira Tokui *et al.*, U.S. Patent Nos. 5,158,861 and 5,258,266.
[5]M. Zuniga *et al.*, Proc. SPIE **2724** (1996).